Cardiovascular Pathology 38 (2019) 1–6

Contents lists available at ScienceDirect

Cardiovascular Pathology

Clinical Case Report

Renal cystic disease in the *Fbn1*$^{C1039G/+}$ Marfan mouse is associated with enhanced aortic aneurysm formation☆

Stijntje Hibender [a], Shaynah Wanga [a], Ingeborg van der Made [b], Mariska Vos [a], Barbara JM Mulder [c], Ron Balm [d], Carlie JM de Vries [a], Vivian de Waard [a,*]

[a] Department of Medical Biochemistry, Amsterdam Cardiovascular Sciences, Amsterdam UMC, Univ of Amsterdam, Meibergdreef 9, Amsterdam, the Netherlands
[b] Department of Experimental Cardiology, Amsterdam Cardiovascular Sciences, Amsterdam UMC, Univ of Amsterdam, Meibergdreef 9, Amsterdam, the Netherlands
[c] Department of Cardiology, Amsterdam UMC, Univ of Amsterdam, Meibergdreef 9, Amsterdam, the Netherlands
[d] Department of Surgery, Amsterdam UMC, Univ of Amsterdam, Meibergdreef 9, Amsterdam, the Netherlands

ARTICLE INFO

Article history:
Received 12 July 2018
Received in revised form 2 October 2018
Accepted 3 October 2018

Keywords:
Cystic kidney
Aneurysm
Marfan Syndrome

ABSTRACT

Marfan syndrome (MFS) is a connective tissue disorder caused by mutations in the fibrillin-1 gene (*FBN1*), resulting in aortic aneurysm formation and dissections. Interestingly, variable aortopathy is observed even within MFS families with the same mutation. Thus, additional risk factors determine disease severity. Here, we describe a case of a 2-month-old *Fbn1*$^{C1039G/+}$ MFS mouse with extreme aortic dilatation and increased vascular inflammation, when compared to MFS siblings, which coincided with unilateral renal cystic disease. In addition, this mouse presented with increased serum levels of creatinine, angiotensin-converting enzyme, corticosterone, macrophage chemoattractant protein-1, and interleukin-6, which may have contributed to the vascular pathology.

Possibly, cystic kidney disease is associated with aneurysm progression in MFS patients. Therefore, we propose that close monitoring of the presence of renal cysts in MFS patients, during regular vascular imaging of the whole aorta trajectory, may provide insight in the frequency of cystic kidney disease and its potential as a novel indicator of aneurysm progression in MFS patients.

1. Introduction

Mutations in the fibrillin-1 gene (*FBN1*) cause Marfan syndrome (MFS), which is an autosomal connective tissue disorder with an incidence of 1–2 per 10,000 individuals [1]. Most MFS patients develop aortic aneurysms with dissections or ruptures as life-threatening consequences. Currently, β-blockers or angiotensin receptor blockers are used to lower blood pressure to reduce aortic aneurysm growth [2,3]. However, predicting adverse aortic events is still challenging. Known risk factors for aortic dissections are mainly related to aortopathy features or pregnancy [4,5].

Here, we present a young *Fbn1*$^{C1039G/+}$ MFS mouse with unilateral cystic kidney disease and extreme aortic aneurysm formation. Renal cysts are commonly observed in the human population; however, renal cysts are even more prevalent in patients with an abdominal aortic aneurysm or a thoracic aortic aneurysm [6,7]. Moreover, in a small abdominal visceral study in MFS patients, 59% of the MFS patients showed renal cysts, in contrast to 30% of non-MFS controls [8]. This reveals that renal cysts occur more often in MFS, which may be related to the role of fibrillin-1 in the kidney [9]. We hypothesize that excessive cystic kidney disease may influence aortic aneurysm development by promoting vascular inflammation.

2. Methods

2.1. Animal studies

Fbn1$^{C1039G/+}$ MFS mice on a C57Bl6 background were used in this study and generated from a heterozygous breeding colony. At 2 months of age, the male index MFS mouse underwent echocardiography, and a cystic kidney was palpated, which was the reason to euthanize. Two male MFS siblings also underwent echocardiography at 2 months of age; however, these mice were euthanized and dissected at 4 months of age. As reference for aneurysm development, the aortic dilatation and distensibility were measured in 2- and 8-month old male wild-type (WT) and MFS mice during echocardiography (n=4–6 per group). The euthanized mice were perfusion-fixed, and heart and aorta were collected. Animal care and experimental procedures were

☆ Sources of funding: Academic Medical Center (AMC) Graduate School (AMC PhD Scholarship; S.H.), AMC Foundation (private funding; R.B.).
* Corresponding author at: Amsterdam UMC, Dept of Medical Biochemistry, K1-115, Meibergdreef 9, 1105 AZ Amsterdam, the Netherlands. Tel.: +31 20 566 5129.
E-mail address: v.dewaard@amc.uva.nl (V. de Waard).

https://doi.org/10.1016/j.carpath.2018.10.002

approved by the independent animal experimental committee for Animal Welfare of the Academic Medical Center in Amsterdam according to the guidelines of the Academic Medical Center and the Directive 2010/63/EU of the European Parliament.

2.2. Echocardiography

To measure the aortic diameter, transthoracic echocardiograms were performed in isoflurane-anesthetized mice (4% isoflurane for induction, 2%–3% isoflurane and O_2 for maintenance of anesthesia) by using the Vevo770 high-resolution imaging system with a 40-MHz probe (RMV 704 scanhead) (VisualSonics Inc., Toronto, Canada). A two-dimensional short-axis view of the aorta was obtained at the level of the aortic root. The average of three aortic measurements per mouse per location was calculated.

2.3. β-Galactosidase staining

Aortic arches, containing the ascending aorta, arch, and proximal thoracic descending aorta, were fixed with 4% neutral buffered formaldehyde (Shandon Formal-Fixx, Thermo Scientific). To visualize vascular inflammation and senescence, the arches were stained for 48 h at 37°C in buffer containing 1 mg/ml 5-bromo-4-chloro-3-indolyl β-D-galactoside (X-Gal) (Invitrogen), 150 mmol/L NaCl, 2 mmol/L $MgCl_2$, 5 mmol/L potassium hexacyanoferrate(III) (244,023, Sigma-Aldrich), 5 mmol/L potassium hexacyanoferrate(II) trihydrate (P3289, Sigma-Aldrich), and 40 mmol/L citric acid/sodium hydrogen phosphate buffer (pH 6). Unspecified chemicals were from Merck.

2.4. Serum measurements

Serum of the MFS mice was analyzed. Creatinine and angiotensin-converting enzyme (ACE) measurements were performed by the Department of Clinical Chemistry at the Academic Medical Center in Amsterdam. Corticosterone was measured by an enzyme-linked immunosorbent assay (Assaypro). To determine macrophage chemoattractant protein-1 (MCP-1) and interleukin-6 (IL-6) levels, the Cytometric Bead Array Mouse Inflammation Kit (BD Biosciences) was used.

2.5. Immunohistochemistry

Murine hearts and ascending aortas were embedded in paraffin and cross-sectioned (7 μm). After deparaffinization and rehydration, hematoxylin and eosin (H&E) staining was performed to visualize nuclei and cytoplasm of the cells. Lawson (Klinipath) staining was performed to visualize the elastic laminae. Immunohistochemical stainings were initiated by quenching endogenous peroxidase activity for 20 min in 1% H_2O_2. Antigen retrieval was performed in citrate buffer pH 6 for the CD45 staining to recognize all leukocytes. Incubation with antibodies recognizing CD45 (eBiosciences, clone 30-F11) or alpha-smooth muscle-actin (a-SMA) (DAKO, 1A4) was followed by washing and incubation with a horseradish peroxidase (HRP)-conjugated anti-rabbit IgG polymer (BrightVision, ImmunoLogic) for CD45 or an HRP-conjugated goat anti-mouse IgG2A antibody (Southern Biotech) for a-SMA. Diaminobenzidine tetrachloride was used as substrate. Hereafter, sections were embedded in Pertex (HistoLab). Microscopic pictures were taken with the Leica Microsystem.

2.6. Statistical analysis

Graphs were made with GraphPad Prism 5 software and represent the mean+S.E.M. Data in text represent mean±S.D. The unpaired Student's *t* test was used. A *P* value ≤.05 was considered significant, represented in the graphs by $^{*}P \leq .05$, $^{**}P \leq .01$, and $^{***}P \leq .001$.

3. Results

3.1. Enhanced aortic dilatation in an MFS mouse with renal cystic disease

From our experience with the *Fbn1*$^{C1039G/+}$ MFS mice, we know that they already show minimal but significant aortic root dilatation at 2 months of age: aortic diameter 1.66±0.07 mm in MFS versus 1.5±0.06 mm in WT mice (n=6 male mice per group; P=.009), as also observed by others [10]. The diameter of the ascending aorta is not significantly different at this age: 1.53±0.06 mm in MFS and 1.44±0.06 mm in WT, respectively (P=.34), and as shown previously [11]. Unexpectedly, we discovered extensive aortic root dilatation (2.64±0.15 mm) and ascending aorta dilatation (2.23±0.09 mm) in a male *Fbn1*$^{C1039G/+}$ MFS mouse at 2 months of age during routine echocardiography (Fig. 1A–C). The 2-month-old MFS siblings displayed aortic root diameters of 1.90±0.10 mm and ascending aorta diameters of 1.69±0.06 mm. The extreme aorta diameters of the index MFS mouse were actually comparable with dilatation that is usually measured in 8-month-old MFS mice [10], as we also observed (n=4; aortic root 2.16±0.26 mm and ascending aorta 2.06±0.14 mm) (Fig. 1A and B). Aortic distensibility of the ascending aorta was reduced considerably in the index MFS mouse: 14% versus 32% in the MFS siblings. Again, the index mouse resembled 8-month-old MFS mice with distensibility of 11%±3% (Fig. 1D), suggesting severe elastic lamina loss.

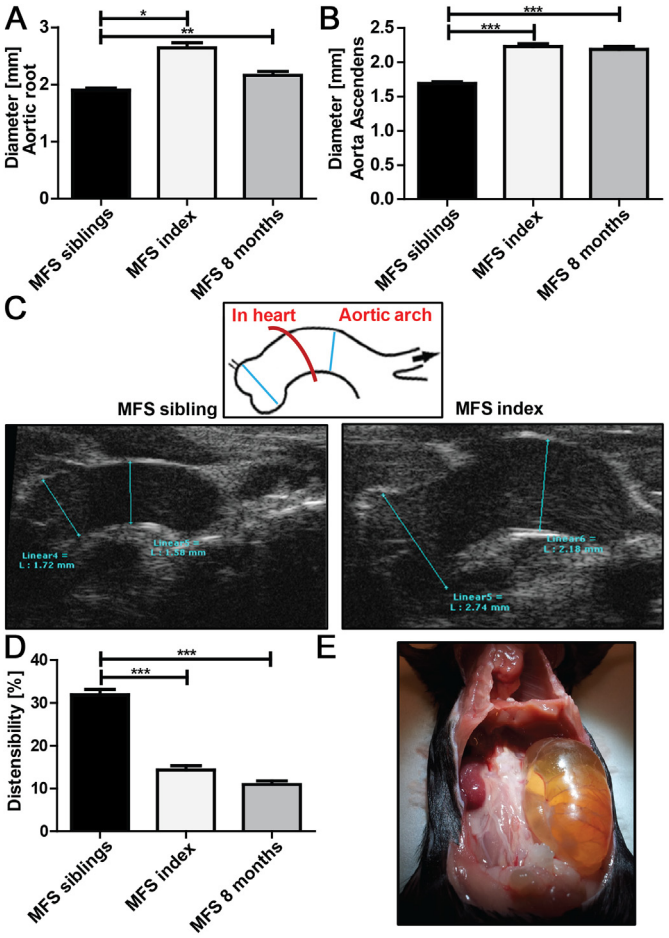

Fig. 1. Echocardiography in 2- and 8-month-old MFS mice. (A) The diameter of the aortic root (mm) and (B) the ascending aorta (mm) in 2-month-old MFS mice (two siblings), the MFS mouse with the cystic kidney (index), and the 8-month-old MFS mice. (C) Two-dimensional short-axis view revealing the sites of aortic measurement during echocardiography and the actual aortic images of the index MFS mouse compared to one of its MFS siblings. (D) Distensibility (%) of the ascending aorta in MFS siblings, the index MFS mouse, and the 8-month old MFS mice. (E) MFS mouse with the unilateral cystic kidney. On the left, the normal kidney size can be appreciated.

The MFS mouse with enhanced aorta dilatation showed signs of distress, and further examination resulted in discovery of a unilateral cystic kidney (Fig. 1E), which we had observed once before in yet another MFS mouse (Fig. S1) but never in WT mice from the same heterozygous MFS breeding colony.

3.2. Aortic aneurysm analysis

Microscopic analysis revealed severe dilatation of the aortic root in the MFS mouse with cystic kidney disease (Fig. 2A). In addition, aortic calcification, inflammation, and hemorrhage were detected in the aortic root. Calcification was observed in the smooth muscle cell-rich medial layer of the aortic wall (Fig. 2B), whereas inflammation (Fig. 2C) and hemorrhage (Fig. 2D) were predominantly present in the adventitial layer surrounding the aortic root, originating from inflammation of vasa vasorum. In addition, the ascending aorta of the index MFS mouse contained more extensive elastin breaks (Fig. 2E).

Macroscopic analysis of the aortic arch revealed a substantial saccular aneurysm at the base of the ascending aorta, which is rather unusual in MFS (Fig. 2F, arrow). The saccular aneurysm is blue since incubation of the aortic arch with X-gal substrate showed that cells located in the saccular aneurysm have excessive beta-galactosidase activity. Macrophages have enhanced beta-galactosidase activity since they contain many lysosomes. After sectioning of the aortic aneurysm and staining for inflammatory cells, we confirmed infiltration of CD45-positive leukocytes (Fig. 3, left panel), suggesting aortitis-induced aneurysm

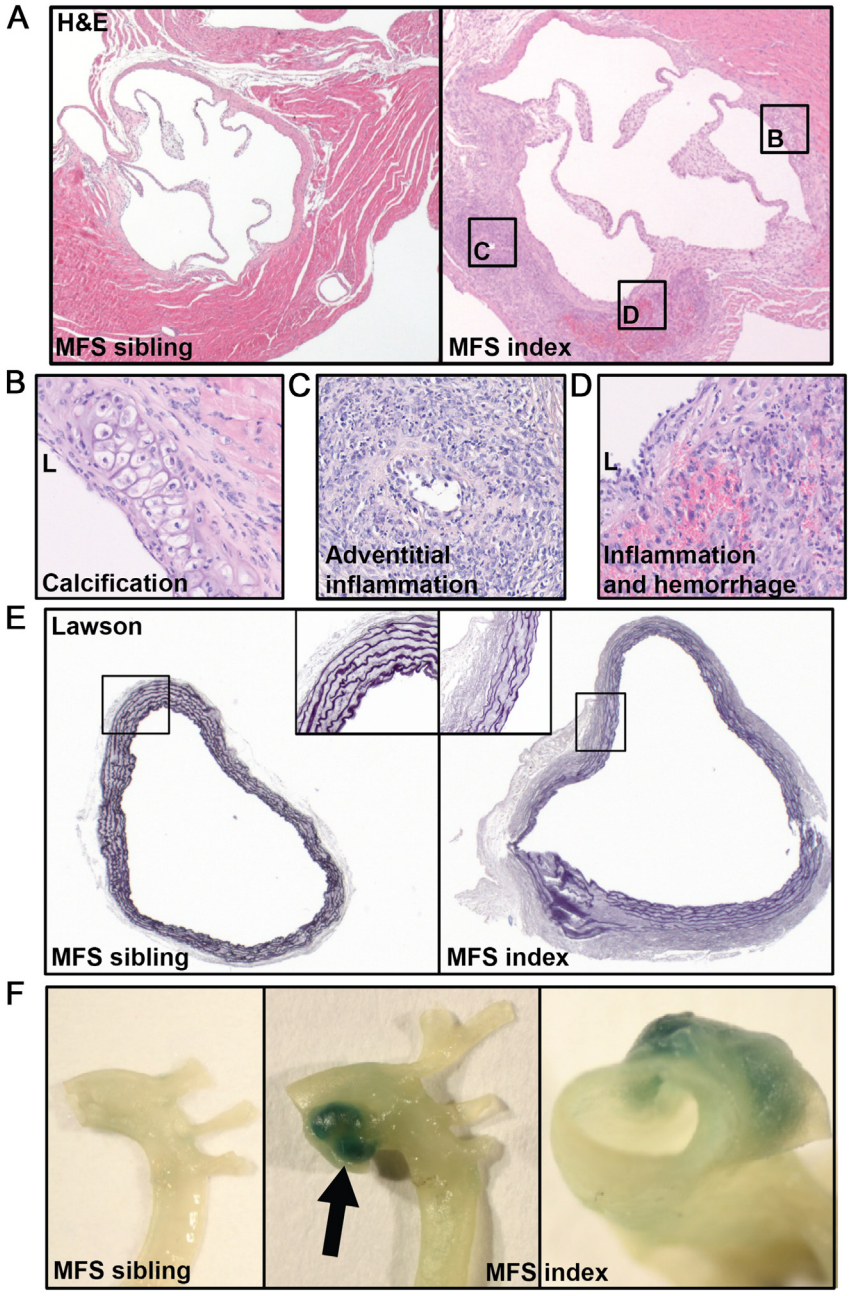

Fig. 2. Aortic root and ascending aorta of MFS mice. (A) H&E-stained aortic root, including valve leaflets, of the index MFS mouse compared to its sibling (magnification: 25×). (B) Calcification in the smooth muscle cell-rich medial layer of the aortic root of the MFS index mouse (200×). (C) Inflammation in the adventitia, localized to the vasa vasorum (200×). (D) Inflammation-induced hemorrhage in the adventitia surrounding the aortic root (200×). (E) Lawson-stained cross sections of the ascending aorta from the index MFS mouse and its sibling (25×, inlays: 200×). (F) Aortic arch of an MFS mouse without (left panel) and with the cystic kidney (middle/right panels). View from the side (middle panel) and from the heart into the ascending aorta (right panel) (6.5× and 10×, respectively). A large saccular aneurysm is observed, which is blue due to staining with X-Gal, to visualize vascular inflammation (macrophages).

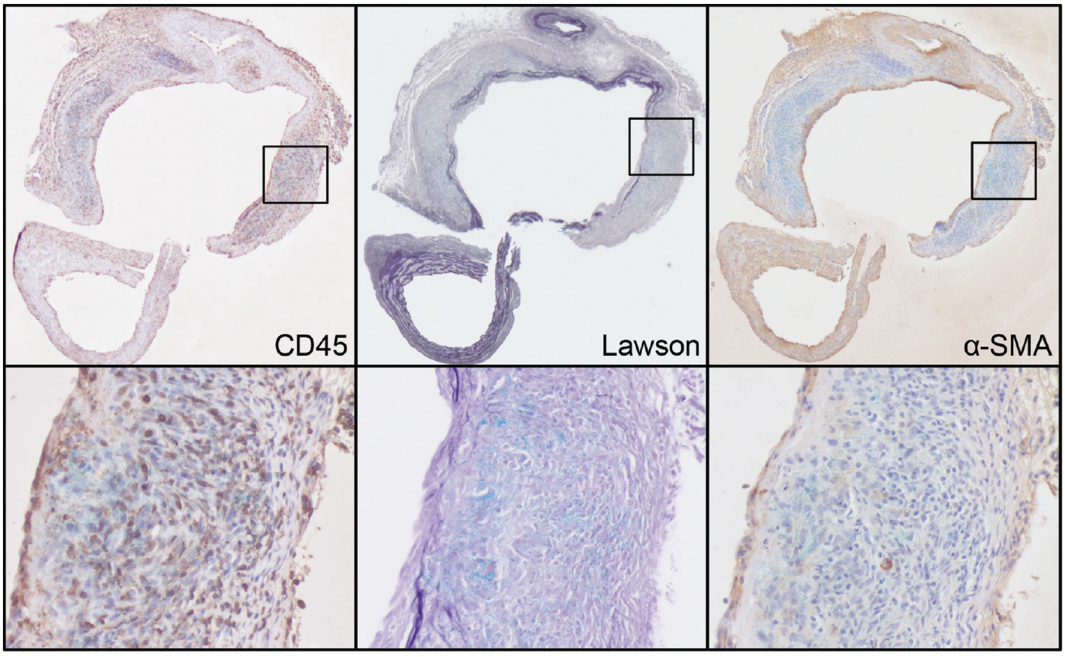

Fig. 3. Saccular aneurysm of the ascending aorta. Cytochemical and immunohistochemical stainings of the saccular aneurysm (magnification: 25× upper panels, 200× lower panels). (Left) Leukocyte staining (CD45; brown) visualizes aortitis. X-Gal-positive cells in the aneurysm are light blue and nuclei are dark blue. (Middle) Lawson staining shows purple elastic laminae, which are almost absent within the saccular aneurysm. X-Gal-positive cells in the aneurysm are light blue. (Right) Smooth muscle cell staining (α-SMA; brown) reveals limited smooth muscle cell presence. The light-blue-stained cells are X-Gal-positive cells, and cell nuclei are dark blue.

formation. However, it cannot be excluded that part of the blue X-gal staining was due to senescent vascular cells since cytoplasmic beta-galactosidase activity is a hallmark of cellular senescence [12] and cellular senescence is reported in vascular disease and aneurysms [13,14], also in the *Fbn1*$^{C1039G/+}$ MFS mice [15].

Severe elastin fragmentation was observed in the saccular aneurysm, and in certain areas, elastin was no longer present (Fig. 3, middle panels), which is presumably caused by excessive proteolytic activity of the inflammatory cells (Fig. 3, left panels). In addition, the medial smooth muscle cell layer was compromised, indicating enhanced smooth muscle cell loss (Fig. 3, right panels).

3.3. Systemic parameters in MFS mice

As measure for kidney function, serum creatinine was analyzed (Table 1). A 1.8-fold increase in serum creatinine levels was observed in the MFS mouse with cystic kidney disease. The low creatinine levels in the MFS siblings seem to support that, under normal circumstances, reduced fibrillin-1 expression does not influence kidney function.

In MFS patients, blood pressure regulation is standard practice to diminish aorta pathology. As a measure for blood pressure regulation, ACE levels were analyzed and were comparable with documented ACE levels in mice [16]. ACE generates the hormonal peptide angiotensin-II, which activates the angiotensin-II receptors. Given that ACE was increased 1.2-fold in the index MFS mouse (Table 1), this may potentially have led to a modest increase in angiotensin-II and consequently in enhanced blood pressure and aortic inflammation, which are known to influence aneurysm formation in mice [17].

We have shown previously that the glucocorticoid methylprednisolone promotes aorta pathology in the *Fbn1*$^{C1039G/+}$ MFS mouse model [18], suggesting that a chronic increase in corticosterone may be harmful. The stress hormone corticosterone was indeed 2.4-fold higher in the index MFS mouse as compared to its siblings (Table 1).

The proinflammatory chemokine MCP-1, as well as cytokine IL-6, is strongly associated with aneurysm formation [19,20]. We observed a 5.4-fold increased level of MCP-1, and the IL-6 concentration was 91 pg/ml in the index MFS mouse, while it was undetectable in the MFS siblings (Table 1). Probably, these cytokines were involved in the recruitment of inflammatory cells to the damaged vascular wall [21].

Table 1
Serum measurements

	MFS siblings	MFS index	Fold induction
Creatinine (μmol/L)	10	19	1.8
ACE (U/L)	374	449	1.2
Corticosterone (ng/ml)	93	219	2.4
MCP-1 (pg/ml)	4	22	5.4
IL-6 (pg/ml)	0	91	

The absolute values and fold increase of serum variables in the index MFS mouse with renal cystic disease and the MFS siblings (average of the two mice).

4. Discussion

In the current study, we presented a case of a young *Fbn1*$^{C1039G/+}$ MFS mouse with a cystic kidney and extreme aneurysm formation in the aortic root and ascending aorta. Interestingly, the augmented aortic dilatation was associated with excessive vascular inflammation, which is unusual in MFS. In addition, a saccular aneurysm was present which most likely was caused by aortitis in the index MFS mouse, as has been presented in an MFS patient once [22]. Aortitis is known to cause saccular aneurysm formation by local destruction of the extracellular matrix and smooth muscle cells [23]. The association of renal cysts and aorta pathology seems relevant since an extensive study including over 500 (non-MFS) aortic dissection patients showed renal cysts in 38% of the patients versus 22% in over 1300 nondissected control patients [24]. Moreover, 59% of MFS patients versus 30% of non-MFS controls presented with renal cysts after an abdominal visceral evaluation [8]. Unfortunately, in the latter study, it was not determined whether MFS patients with renal cysts showed enhanced aneurysm growth.

The relationship between renal cysts and aneurysm formation is already established in a genetic form of cystic kidney disease in patients with autosomal dominant polycystic kidney disease (ADPKD). ADPKD is caused by mutations in the polycystin genes (*PKD1* and *2*) [25]. This disease is associated with aneurysm formation and ruptures in

intracerebral arteries, causing stroke. Patients with ADPKD have a 12% risk to develop cerebral aneurysms, which is even higher (22%) in patients with a family history in aneurysm formation [26]. In ADPKD patients, aortic aneurysms and dissections occur occasionally and seem related to the PKD mutation [27,28]. In mice heterozygous for both *Pkd1* and *Fbn1*, excessive elastin fragmentation has been observed in the aorta when compared to mice just deficient for *Pkd1* [29]. This study revealed that the MFS aortic phenotype was aggravated in an ADPKD background. However, in that study, aortic dilatation was not determined.

While the kidneys we observed in the two affected MFS mice showed signs of hydronephrosis, we were unable to pinpoint the underlying cause of the susceptibility to develop cysts. In the current study, we observed enhanced ACE, glucocorticoids, and chemokines/interleukins in the MFS mouse with the renal cyst, which could be involved in aneurysm disease.

ACE polymorphisms, enhancing ACE activity, have been associated with aneurysm development in human patients [30]. In mice, the most well-known model to induce aortic aneurysms and dissections throughout the whole aortic trajectory is infusion of angiotensin-II, the downstream target of ACE. Angiotensin-II causes an increase in blood pressure, but more importantly, it causes aortic inflammation [17]. Additional support for involvement of this pathway is underlined by the association of angiotensin receptor type-1 (AGTR1) polymorphisms with aneurysm development [30]. Interestingly, AGTR1 deficiency only in endothelial cells abrogates aneurysm development in the mgR/mgR MFS mouse model [31]. Moreover, chronic angiotensin-II infusion into *Fbn1*$^{C1039G/+}$ MFS mice accelerates aortopathy [32], and blockade of AGTR1 with the blood-pressure-lowering drug losartan inhibits aneurysm formation in this MFS model [10] and also in a subset of MFS patients [33], suggesting a role for this pathway in MFS.

Blotchy mice, with a connective tissue defect in collagen/elastin cross-linking, develop spontaneous aortic aneurysms and dissections. Providing hydrocortisone in their drinking water increased the incidence of aneurysms and fatal ruptures [34]. In addition, our previous data in the *Fbn1*$^{C1039G/+}$ MFS mice show a detrimental effect of chronic methylprednisolone treatment on aorta pathology [18]. In line with these data, activation of the mineralocorticoid receptor (a nuclear receptor sensitive to mineralocorticoids and glucocorticoids) induces aortic aneurysm formation and rupture in the presence of high salt in WT mice, despite blood pressure lowering [35]. Glucocorticoids are widely used in the clinic as immunosuppressive drugs, and there is evidence in human transplant patients that the prolonged use of glucocorticoids may be causally related to enhanced aneurysm progression [36,37], presumably by affecting aortic smooth muscle cell repair. While it is clear that inflammation is excessive in abdominal aneurysms, aneurysms in MFS patients have very limited inflammation and are related to intrinsic extracellular matrix defects. Yet, enhanced aortic inflammation may aggravate aortopathy in MFS.

A relevant role for inflammation is illustrated by inhibition of MCP-1 or its receptor, chemokine (C-C motif) receptor 2 (CCR2), which prevented aneurysm formation in different mouse models by decreasing inflammation [21,38,39]. Interestingly, there is an IL-6/MCP-1 vascular inflammation loop, promoting thoracic and abdominal aortic aneurysm formation and dissections, which was prevented in either CCR2- or IL-6-deficient mice [38]. Likewise, chronic infusion of IL-6 induced aortic dilatation and inflammation via MCP-1 [40]. In line with these data, aneurysm formation was reduced by inhibition of IL-6 signaling (with antibody therapy) or IL-6 deficiency in mice [41,42]. Also in the mgR/mgR MFS mouse model, deficiency of IL-6 decreased aortic dilatation [43]. Intriguingly, the role of the IL-6/MCP1-axis is not entirely clear since blockade of only leukocyte CCR2 inhibited aneurysm formation, while whole-body CCR2 blockade by mutant MCP1-7ND protein enhanced aneurysm progression in the angiotensin-II-induced aneurysm model [21]. Similarly, blockade of IL-6 after onset of aneurysm formation inhibited aneurysm progression, while blockade of IL-6 just prior to aneurysm formation enhanced aortic rupture in the elastase-induced aneurysm model [44]. While MCP-1 and IL-6 are important inflammatory mediators, they also promote wound healing by activation of nonimmune cells, which would explain the discrepancies observed [21,45] and the difficulty with anti-inflammatory drugs as treatment strategy.

Taken together, from the two descriptive murine MFS cystic kidney disease cases demonstrated here and the existing literature, there seem abundant clues that cystic kidney disease may be causally involved in the pathogenesis of aortic aneurysm formation by promoting aortic inflammation. Yet, it may also represent a subgroup of MFS patients who are predisposed to develop cystic kidney disease and aneurysms, and as such serves as a valuable marker for aortic risk assessment. Therefore, we propose that close monitoring of the presence of renal cysts in aneurysm patients during regular vascular imaging of the whole aorta trajectory may provide insight in the frequency of renal cystic disease and its potential as a novel marker of and/or target against aneurysm progression in MFS patients.

Supplementary data to this article can be found online at https://doi.org/10.1016/j.carpath.2018.10.002.

Acknowledgments

We thank Dr. M. Gijbels (Department of Medical Biochemistry) for her contribution to the histopathological analysis, Dr. J.P. van Straalen (Department of Clinical Chemistry) for his technical assistance, and Prof. S. Florquin (Department of Pathology) for the critical discussions.

References

[1] Judge DP, Dietz HC. Marfan's syndrome. Lancet 2005;366(2):247–54. https://doi.org/10.1016/S0140-6736(05)67789-6.
[2] Gao L, Chen L, Fan L, Gao D, Liang Z, Wang R, et al. The effect of losartan on progressive aortic dilatation in patients with Marfan's syndrome: a meta-analysis of prospective randomized clinical trials. Int J Cardiol 2016;217:190–4. https://doi.org/10.1016/j.ijcard.2016.04.186.
[3] Franken R, Mulder BJ. Aortic disease: Losartan versus atenolol in the Marfan aorta-how to treat? Nat Rev Cardiol 2015;12(8):447–8. https://doi.org/10.1038/nrcardio.2015.95.
[4] Wanga S, Silversides CK, Dore A, de Waard V, Mulder BJM. Pregnancy and thoracic aortic disease—managing the risks. Can J Cardiol 2015. https://doi.org/10.1016/j.cjca.2015.09.003.
[5] den Hartog AW, Franken R, Zwinderman AH, Timmermans J, Scholte AJ, van den Berg MP, et al. The risk for type B aortic dissection in Marfan syndrome. J Am Coll Cardiol 2015;65(3):246–54. https://doi.org/10.1016/j.jacc.2014.10.050.
[6] Takagi H, Umemoto T. Simple renal cyst and abdominal aortic aneurysm. J Vasc Surg 2016;63:254–9. https://doi.org/10.1016/j.jvs.2015.08.095.
[7] Ziganshin BA, Theodoropoulos P, Salloum MN, Zaza KJ, Tranquilli M, Mojibian HR, et al. Simple renal cysts as markers of thoracic aortic disease. J Am Heart Assoc 2016;5:e002248. https://doi.org/10.1161/JAHA.115.002248.
[8] Chow K, Pyeritz RE, Litt HI. Abdominal visceral findings in patients with Marfan syndrome. Genet Med 2007;9(4):208–12 [doi:10.1097GIM.0b013e3180423cb3].
[9] Schaefer L, Mihalik D, Babelova A, Krzyzankova M, Gröne HJ, Iozzo RV, et al. Regulation of fibrillin-1 by biglycan and decorin is important for tissue preservation in the kidney during pressure-induced injury. Am J Pathol 2004;165(2):383–96. https://doi.org/10.1016/S0002-9440(10)63305-6.
[10] Habashi JP, Judge DP, Holm TM, Cohn RD, Loeys BL, Cooper TK, et al. Losartan, an AT1 antagonist, prevents aortic aneurysm in a mouse model of Marfan syndrome. Science 2006;312(5770):117–21. https://doi.org/10.1126/science.1124287.
[11] Holm TM, Habashi JP, Doyle JJ, Bedja D, Chen Y, van Erp C, et al. Noncanonical TGFβ signaling contributes to aortic aneurysm progression in Marfan syndrome mice. Science 2011;332(6027):358–61. https://doi.org/10.1126/science.1192149.
[12] Campisi J. Senescent cells, tumor suppression, and organismal aging: good citizens, bad neighbors. Cell 2005;120(4):513–22. https://doi.org/10.1016/j.cell.2005.02.003.
[13] Kovacic JC, Moreno P, Hachinski V, Nabel EG, Fuster V. Cellular senescence, vascular disease, and aging: part 1 of a 2-part review. Circulation 2011;123(15):1650–60. https://doi.org/10.1161/CIRCULATIONAHA.110.007021.
[14] Riches K, Angelini TG, Mudhar GS, Kaye J, Clark E, Bailey MA, et al. Exploring smooth muscle phenotype and function in a bioreactor model of abdominal aortic aneurysm. J Transl Med 2013;11(1):208. https://doi.org/10.1186/1479-5876-11-208.
[15] Hibender S, Franken R, van Roomen C, Ter Braake A, van der Made I, Schermer EE, et al. Resveratrol inhibits aortic root dilatation in the Fbn1C1039G/+ Marfan mouse model. Arterioscler Thromb Vasc Biol 2016;36:1618–26. https://doi.org/10.1161/ATVBAHA.116.307841.
[16] Esther CR, Marino EM, Howard TE, Machaud A, Corvol P, Capecchi MR, et al. The critical role of tissue angiotensin-converting enzyme as revealed by gene targeting in mice. J Clin Invest 1997;99(10):2375–85. https://doi.org/10.1172/JCI119419.

[17] Lu H, Rateri DL, Bruemmer D, Cassis LA, Daugherty A. Involvement of the renin-angiotensin system in abdominal and thoracic aortic aneurysms. Clin Sci (Lond) 2012;123(9):531–43. https://doi.org/10.1042/CS20120097.
[18] Franken R, Hibender S, den Hartog AW, Radonic T, de Vries CJ, Zwinderman AH, et al. No beneficial effect of general and specific anti-inflammatory therapies on aortic dilatation in Marfan mice. PLoS One 2014;9(9):e107221. https://doi.org/10.1371/journal.pone.0107221.
[19] Lindeman JHN, Abdul-Hussien H, Schaapherder AFM, Van Bockel JH, Von der Thüsen JH, Roelen DL, et al. Enhanced expression and activation of pro-inflammatory transcription factors distinguish aneurysmal from atherosclerotic aorta: IL-6- and IL-8-dominated inflammatory responses prevail in the human aneurysm. Clin Sci 2008; 114(11):687–97. https://doi.org/10.1042/CS20070352.
[20] Harrison SC, Smith AJP, Jones GT, Swerdlow DI, Rampuri R, Bown MJ, et al. Interleukin-6 receptor pathways in abdominal aortic aneurysm. Eur Heart J 2013; 34(48):3707–16. https://doi.org/10.1093/eurheartj/ehs354.
[21] de Waard V, Bot I, de Jager SCA, Talib S, Egashira K, de Vries MR, et al. Systemic MCP1/CCR2 blockade and leukocyte specific MCP1/CCR2 inhibition affect aortic aneurysm formation differently. Atherosclerosis 2010;211(1):84–9. https://doi.org/10.1016/j.atherosclerosis.2010.01.042.
[22] Cordera F, Bowen JM, Aubry MC, Gloviczki P. Type IV thoracoabdominal aortic aneurysm with lymphoplasmacytic aortitis and cystic medial degeneration in a 32-year-old patient with Marfan syndrome. J Vasc Surg 2005;42:168–71. https://doi.org/10.1016/j.jvs.2005.03.033.
[23] Gornik HL, Creager MA. Aortitis. Circulation 2008;117:3039–51. https://doi.org/10.1161/CIRCULATIONAHA.107.760686.
[24] Kim EK, Choi ER, Song BG, Jang SY, Ko SM, Choi SH, et al. Presence of simple renal cysts is associated with increased risk of aortic dissection: a common manifestation of connective tissue degeneration? Heart 2011;97(1):55–9. https://doi.org/10.1136/hrt.2010.205328.
[25] Ong ACM, Harris PC. A polycystin-centric view of cyst formation and disease: the polycystins revisited. Kidney Int 2015:1–12. https://doi.org/10.1038/ki.2015.207.
[26] Xu HW, Yu SQ, Mei CL, Li MH. Screening for intracranial aneurysm in 355 patients with autosomal-dominant polycystic kidney disease. Stroke 2011;42:204–6.
[27] Sung PH, Yang YH, Chiang HJ, Chiang JY, Chen CJ, Liu CT, et al. Risk of aortic aneurysm and dissection in patients with autosomal-dominant polycystic kidney disease: a nationwide population-based cohort study. Oncotarget 2017;8(34):57594–604. https://doi.org/10.18632/oncotarget.16338.
[28] Zhang W, Han Q, Liu Z, Zhou W, Cao Q, Zhou W. Whole exome sequencing reveals a stop-gain mutation of PKD2 in an autosomal dominant polycystic kidney disease family complicated with aortic dissection. BMC Med Genet 2018;19(1):19. https://doi.org/10.1186/s12881-018-0536-6.
[29] Liu D, Wang CJ, Judge DP, Halushka MK, Ni J, Habashi JP, et al. A Pkd1-Fbn1 genetic interaction implicates TGF-β signaling in the pathogenesis of vascular complications in autosomal dominant polycystic kidney disease. J Am Soc Nephrol 2014;25(1): 81–91. https://doi.org/10.1681/ASN.2012050486.
[30] Bradley DT, Badger SA, McFarland M, Hughes AE. Abdominal aortic aneurysm genetic associations: mostly false? A systematic review and meta-analysis. Eur J Vasc Endovasc Surg 2016;51(1):64–75. https://doi.org/10.1016/j.ejvs.2015.09.006.
[31] Galatioto J, Caescu CI, Hansen J, Cook JR, Miramontes I, Iyengar R, et al. Cell type-specific contributions of the angiotensin II type 1a receptor to aorta homeostasis and aneurysmal disease-brief report. Arterioscler Thromb Vasc Biol 2018;38(3): 588–91. https://doi.org/10.1161/ATVBAHA.117.310609.
[32] Cavanaugh NB, Qian L, Westergaard NM, Kutschke WJ, Born EJ, Turek JW. A novel murine model of Marfan syndrome accelerates aortopathy and cardiomyopathy. Ann Thorac Surg 2017;104(2):657–65. https://doi.org/10.1016/j.athoracsur.2016.10.077.
[33] Franken R, Den Hartog AW, Radonic T, Micha D, Maugeri A, van Dijk FS, et al. Beneficial outcome of losartan therapy depends on type of FBN1 mutation in Marfan syndrome. Circ Cardiovasc Genet 2015;8:383–8. https://doi.org/10.1161/CIRCGENETICS.114.000950.
[34] Reilly J, Savage E, Brophy C, Tilson M. Hydrocortisone rapidly induces aortic rupture in a genetically susceptible mouse. Arch Surg 1990;125(6):707–9. https://doi.org/10.1001/archsurg.1990.01410180025004.
[35] Liu S, Xie Z, Daugherty A, Cassis LA, Pearson KJ, Gong MC, et al. Mineralocorticoid receptor agonists induce mouse aortic aneurysm formation and rupture in the presence of high salt. Arterioscler Thromb Vasc Biol 2013;33(7):1568–79. https://doi.org/10.1161/ATVBAHA.112.300820.
[36] Lindeman JHN, Rabelink TJ, van Bockel JH. Immunosuppression and the abdominal aortic aneurysm: Doctor Jekyll or Mister Hyde? Circulation 2011;124(18):e463–5. https://doi.org/10.1161/CIRCULATIONAHA.110.008573.
[37] Englesbe MJ, Wu AH, Clowes AW, Zierler RE. The prevalence and natural history of aortic aneurysms in heart and abdominal organ transplant patients. J Vasc Surg 2003;37(1):27–31. https://doi.org/10.1067/mva.2003.57.
[38] Tieu BC, Lee C, Sun H, Lejeune W, Recinos 3rd A, Ju X, et al. An adventitial IL-6/MCP1 amplification loop accelerates macrophage-mediated vascular inflammation leading to aortic dissection in mice. J Clin Invest 2009;119(12):3637–51. https://doi.org/10.1172/JCI38308.
[39] Moehle C, Bhamidipati C, Alexander M, Mehta GS, Irvine JN, Salmon M, et al. Bone marrow-derived MCP1 required for experimental aortic aneurysm formation and smooth muscle phenotypic modulation. J Thorac Cardiovasc Surg 2011;142(6): 1567–74. https://doi.org/10.1016/j.jtcvs.2011.07.053.
[40] Akerman AW, Stroud RE, Barrs RW, Grespin RT, McDonald LT, LaRue RA, et al. Elevated wall tension initiates Interleukin-6 expression and abdominal aortic dilation. Ann Vasc Surg 2018;46:193–204. https://doi.org/10.1016/j.avsg.2017.10.001.
[41] Nishihara M, Aoki H, Ohno S, Furusho A, Hirakata S, Nishida N, et al. The role of IL-6 in pathogenesis of abdominal aortic aneurysm in mice. PLoS One 2017;12(10): e0185923. https://doi.org/10.1371/journal.pone.0185923.
[42] Pope NH, Salmon M, Johnston WF, Lu G, Lau CL, Upchurch Jr GR, et al. Interleukin-6 receptor inhibition prevents descending thoracic aortic aneurysm formation. Ann Thorac Surg 2015;100(5):1620–6. https://doi.org/10.1016/j.athoracsur.2015.05.009.
[43] Ju X, Ijaz T, Sun H, Lejeune W, Vargas G, Shilagard T, et al. IL-6 regulates extracellular matrix remodeling associated with aortic dilation in a fibrillin-1 hypomorphic mgR/mgR mouse model of severe Marfan syndrome. J Am Heart Assoc 2014;3(1): e000476. https://doi.org/10.1161/JAHA.113.000476.
[44] Kokje VBC, Gäbel G, Koole D, Northoff BH, Holdt LM, Hamming JF, et al. IL-6: a Janus-like factor in abdominal aortic aneurysm disease. Atherosclerosis 2016;251:139–46. https://doi.org/10.1016/j.atherosclerosis.2016.06.021.
[45] Hosaka K, Rojas K, Fazal HZ, Schneider MB, Shores J, Federico V, et al. Monocyte chemotactic protein-1–interleukin-6–osteopontin pathway of intra-aneurysmal tissue healing. Stroke 2017;48(4):1052–60. https://doi.org/10.1161/STROKEAHA.116.015590.